Hindawi Publishing Corporation
Journal of Chemistry
Volume 2016, Article ID 5284259, 8 pages
http://dx.doi.org/10.1155/2016/5284259

Research Article

Simple One-Step Method to Synthesize Polypyrrole-Indigo Carmine-Silver Nanocomposite

Lara Fernandes Loguercio,[1,2] Pedro Demingos,[2] Luiza de Mattos Manica,[2] Jordana Borges Griep,[1,2] Marcos José Leite Santos,[1,2] and Jacqueline Ferreira[1,2]

[1]*Programa de Pós-Graduação em Química, Instituto de Química, Universidade Federal do Rio Grande do Sul, 91501-970 Porto Alegre, RS, Brazil*
[2]*Laboratório de Materiais Aplicados e Interfaces, Instituto de Química, Universidade Federal do Rio Grande do Sul, 91501-970 Porto Alegre, RS, Brazil*

Correspondence should be addressed to Jacqueline Ferreira; jacqueline.ferreira@ufrgs.br

Received 9 December 2015; Accepted 31 January 2016

Academic Editor: Frederic Dumur

A nanocomposite of indigo carmine doped polypyrrole/silver nanoparticles was obtained by a one-step electrochemical process. The nanocomposite was characterized by scanning electron microscopy, infrared spectroscopy, ultraviolet-visible-near infrared spectroscopy, and cyclic voltammetry. The simple one-step process allowed the growth of silver nanoparticles during the polymerization of polypyrrole, resulting in films with electrochromic behavior and improved electroactivity. In addition, polypyrrole chains in the nanocomposite were found to present longer conjugation length than pristine polypyrrole films.

1. Introduction

Metallic nanoparticles of silver and gold have been extensively studied due to their optical, electrochemical, and electronic properties [1–3]. During the synthesis and the application of metallic nanoparticles, one should be concerned about agglomeration; hence surface coating is required. Within the last decades many stabilizing species have been studied including molecules with carboxylic acids, thiol groups, inorganic materials, conventional polymers, and conducting polymers [4–9]. According to the literature, in addition to providing stabilization against agglomeration, the use of conducting polymers results in nanocomposites presenting enhanced electrical and electrochemical properties, improved conductivity, robustness, stability, and electrocatalytic activity [10, 11]. Due to their enhanced physical-chemical and biological properties, metal-polymer nanocomposites have been applied in a wide range of areas, such as catalysis, sensors, medicine, and electronics [4, 9].

Among all of the studied metal-conducting polymer nanocomposites, polypyrrole (PPy)-silver nanoparticles (Ag_{nanop}) come to light as a very interesting material; PPy presents environmental stability and high conductivity and can be easily obtained [12–15]. In addition, PPy presents well characterized electrochromic behavior due to the tunable nature of the highest occupied molecular orbital and the lowest unoccupied molecular orbital, which allows for the modulation of its optical and electrical properties [11]. The oxidation of the polymer chain is accompanied by the generation of charges in PPy chain, *polaron* and *bipolaron* states (stabilized local distortions of the backbone), and by the presence of counter ions (dopants). Within the last 30 years many dopants have been studied including organic species, which are found to result in PPy films with improved electrical and optical properties [11, 16, 17]. Indigo carmine is a dianionic dye that acts as an interesting organic dopant once it presents inherent electrochromism, well-known redox mechanism, and a high extinction coefficient [11, 18, 19].

The literature describes a wide range of chemical and electrochemical procedures to synthesize PPy-Ag_{nanop} nanocomposites; for example, Babu and colleagues obtained PPy-Ag_{nanop} nanocomposites by *in situ* chemical polymerization

through a redox reaction between pyrrole and silver nitrate [9]; Wei and colleagues synthesized PPy-Ag_{nanop} nanocomposites at the interface of water and ionic liquid using a one-step UV-induced polymerization [20] and Gupta and colleagues electrodeposited PPy-Ag_{nanop} nanocomposite onto glassy carbon electrode by potentiodynamic polymerization followed by electrodeposition of silver [21]. Among all of the different methodologies, the electrochemical procedures present the advantage of improved synthesis once the electrodeposited components are finely controlled by the solution composition, applied potential, and time [21].

In this work, we show a very simple method to obtain nanocomposites, by growing silver nanoparticles during *in situ* electropolymerization of indigo carmine doped polypyrrole films. We have studied the effects of silver nanoparticles on the optical and electrochemical properties of the nanocomposite, in addition to the electrochromic and the electrocatalytic activity for I_3^-/I^- redox couple. The nanocomposite was characterized by scanning electron microscopy (SEM), cyclic voltammetry (CV), attenuated total reflection, Fourier transform infrared spectroscopy (ATR-FTIR), and ultraviolet-visible-near infrared (UV-VIS-NIR) spectroscopy.

2. Materials and Methods

2.1. Materials. Pyrrole (Aldrich) was distilled and stored at *ca.* 4°C. Indigo carmine, silver nitrate, anhydrous lithium perchlorate, sodium iodate, and iodine (Aldrich) were used as received. All aqueous solutions were prepared with ultrapure water (Milli-Q). Acetonitrile was used to characterize the electrocatalytic activity of the polymeric films.

2.2. Synthesis of PPy-IC-Ag_{nanop} Nanocomposite Film. The electropolymerization of PPy-IC-Ag_{nanop} films (1 cm^2) was carried out in a galvanostat/potentiostat Autolab 302N, using a conventional three-electrode cell. The temperature was controlled at 10°C by using a thermostat Tecnal [11, 22, 23]. Fluorine doped tin oxide substrates (FTO-glass, Solaronix, 15 $\Omega\,cm^{-2}$) were used as working electrode, platinum plate (1 cm^2) was used as counter electrode, and Ag/AgCl was used as reference electrode. The film thickness was controlled with three voltammetric cycles performed from −0.3 to +1.3 V at a scan rate of 30 mV s^{-1}. The solution used for the synthesis was 0.1 mol L^{-1} of pyrrole, 5.0 mmol L^{-1} of indigo carmine, and 6.0 mmol L^{-1} of $AgNO_3$.

2.3. Characterization and Measurements. Infrared spectroscopy was performed in Attenuated Total Reflectance mode using a Bruker model Alpha-P. Optical and spectroelectrochemical measurements were performed in a Perkin Elmer Lambda 25 spectrophotometer and in a galvanostat/potentiostat Autolab 302N. A quartz cuvette was used to assemble the three-electrode cell. Double step potentials of −0.2 and +0.7 V were applied during the electrochromic characterization for a period of 90 seconds [11, 24]. Morphological characterization was performed by scanning electron microscopy using an EVO50 Carl Zeiss microscope at 15 kV.

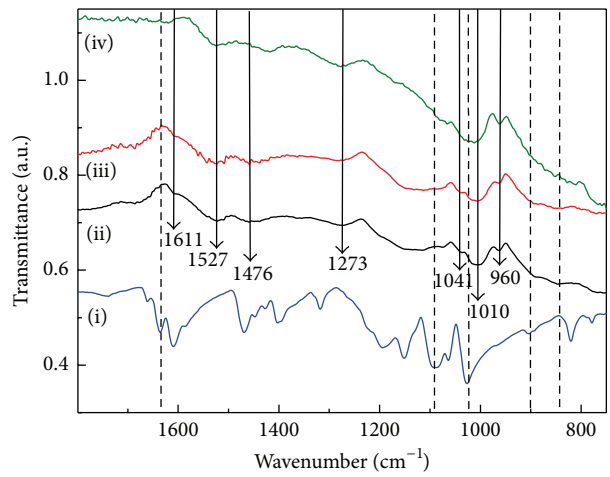

Figure 1: FTIR spectra of (i) pristine IC, (ii) PPy-IC, (iii) PPy-IC-Ag_{nanop}, and (iv) PPy.

Cyclic voltammetry experiments were performed within a potential range from −1.0 to +1.2 V at different scan rates (20, 50, 100, 150, and 200 mV s^{-1}). A 0.1 mol L^{-1} of $LiClO_4$ solution was used as electrolyte. The electrocatalytic activity for I^-/I_3^- redox couple was evaluated with cyclic voltammetry experiments within a potential range from −0.6 to +1.3 V at 20 mV s^{-1}. The electrolyte solution was prepared with 10.0 mmol L^{-1} NaI, 1.0 mmol L^{-1} I_2, and 0.1 mol L^{-1} of $LiClO_4$ in acetonitrile [25].

3. Results and Discussion

3.1. Structural Characterization. Figure 1 shows the FTIR spectra of IC, PPy-IC, and PPy-IC-Ag_{nanop} acquired within the range from 1800 to 750 cm^{-1}. The characteristic vibrational modes of PPy, related to N-H stretch, C-H, N-H, and C-N-C can be observed at 1527, 1010, and 960 cm^{-1}, respectively [11, 16]. The bands at *ca.* 1611, 1476, 1273, and 1041 cm^{-1} are assigned to C=C, C-C, C=N, and C-N stretching and vibration modes of the PPy ring [26–28].

The presence of IC molecules as dopant in PPy-IC and PPy-IC-Ag_{nanop} films is evidenced by the vibrational modes at 1630, 1094, 1026, 900, and 843 cm^{-1} (dashed lines in Figure 1) assigned to C=O, C-O, C-N-C, S-O, and sulphonate anion, respectively [11, 19, 29]. The absence of the vibrational mode at *ca.* 1381 cm^{-1} related to N-O stretching of NO_3^- (present in the silver precursor) strongly suggests that IC molecules are the main species in the doping process [4, 28]. In order to evaluate the effect of silver nanoparticle on the conjugation length of PPy, the ratio between the peak areas at *ca.* 1476 and 1527 cm^{-1} was determined [3, 24, 25]. The nanocomposite presented 1476/1527 cm^{-1} ratio of 0.47 against 0.57 from PPy-IC, and according to a previous study, the smaller ratio suggests that PPy-IC-Ag_{nanop} presents longer effective conjugation length than PPy-IC [11, 26–28].

3.2. Surface Morphology Analysis. Previous works developed by our group [11] demonstred that PPy films doped with

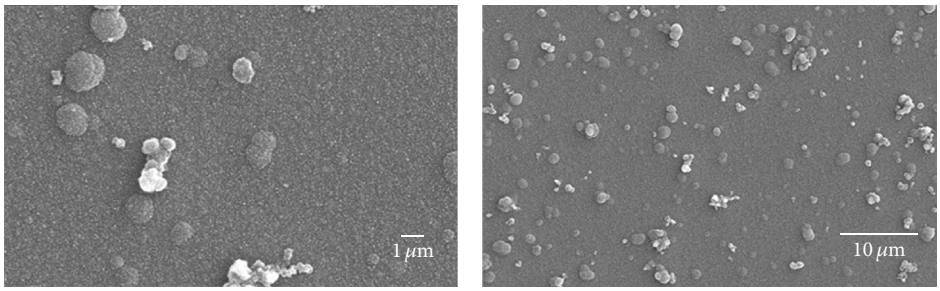

FIGURE 2: SEM images of PPy-IC-Ag_{nanop} film.

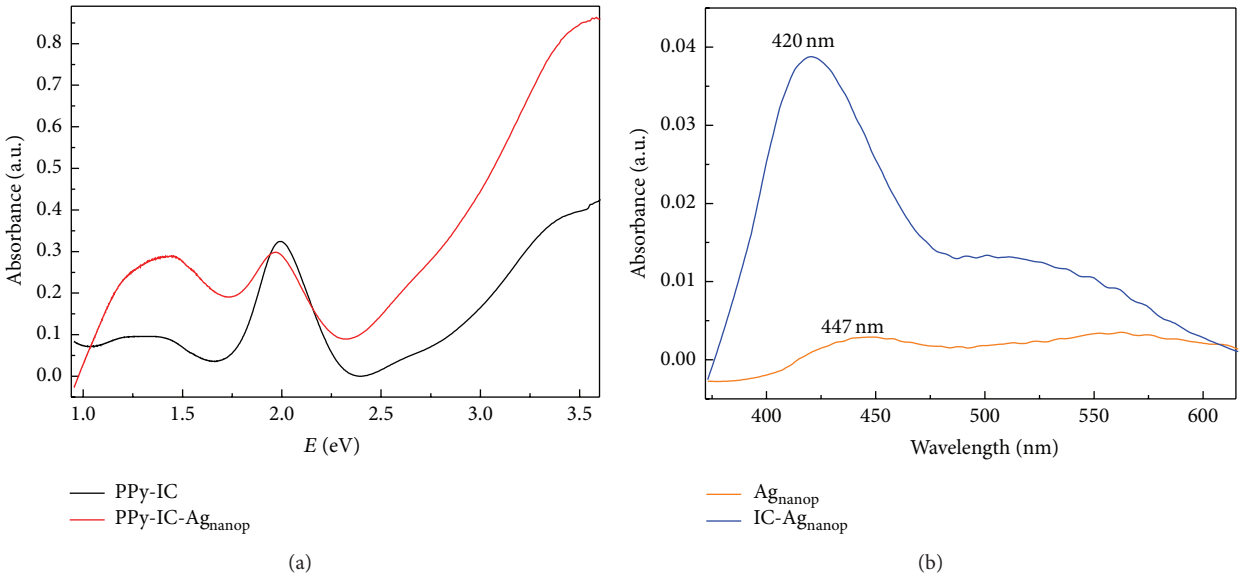

FIGURE 3: UV-VIS-NIR absorption spectra of (a) PPy-IC and PPy-IC-Ag_{nanop} films and (b) Ag_{nanop} and IC-Ag_{nanop} films.

IC molecules present morphology characterized by the formation of very tiny globules, which was found to result in very homogeneous surfaces. Interestingly, the nanocomposite presented the formation of large agglomerates (Figure 2), suggesting the growth of the polymer chains around the silver nanoparticles [30].

3.3. Optical Characterization. Figure 3(a) shows the absorption spectra of PPy-IC and PPy-IC-Ag_{nanop} films. The absorption bands at 3.5, 2.0, and 1.3 eV are related to valence band-conduction band (π-π^*), valence band-antibonding polaron (π-P^*), and polaron-antibonding polaron (P-P^*) electronic transitions, respectively [31–36]. Concerning the position and intensity of these absorption modes, similar doping levels are expected for PPy-IC and PPy-IC-Ag_{nanop}. Due to the strong absorption modes of PPy, the extinction modes characteristic of the silver nanoparticles were not observed (Figure 3(a)); therefore new syntheses of silver nanoparticles were performed using the same conditions, however in the absence of the monomer, using (i) only $AgNO_3$ (Ag_{nanop}) and (ii) IC and $AgNO_3$ (IC-Ag_{nanop}) in the electrolyte (Figure 3(b)). The extinction bands at *ca.* 420 and 447 nm are assigned to the localized surface plasmon resonance (LSPR) characteristic of the silver nanoparticles [37]. The results clearly show that a larger concentration of Ag nanoparticles is formed in the presence of indigo carmine, which can act as stabilizing agent. Hence, the results presented in Figure 3(b) strongly suggest that silver nanoparticles shall be present in PPy-IC-Ag_{nanop}; however, comparing Figures 3(a) and 3(b) one can observe that IC-Ag_{nanop} presents a much weaker absorbance than PPy-IC-Ag_{nanop}; therefore the plasmonic extinction (420 nm, 2.95 eV) is overlapped by the absorption of polypyrrole in the nanocomposite.

3.4. Electrochemical Characterization of PPy-IC and PPy-IC-Ag_{nanop} Films. Figure 4 shows the voltammograms of PPy-IC and PPy-IC-Ag_{nanop} films. One can observe shifts in the electrochemical response of the nanocomposite, in addition to an increase in charge density (*ca.* 119% higher). The interaction between IC molecules and silver nanoparticles may affect the mobility of the dopant inside the polymer matrix, resulting in an increase of the external voltage necessary for the redox process [11, 38]. Charge density is related to charge accumulation at the polymer|solution interface, the presence of silver nanoparticles provides larger surface area for charge accumulation, and in addition, the adsorption

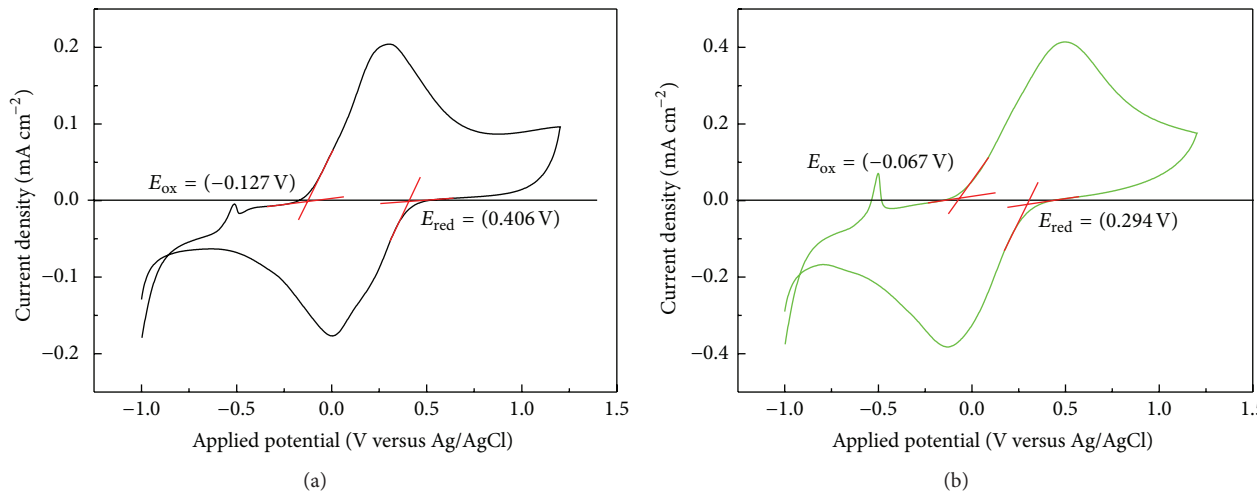

FIGURE 4: Voltammograms of (a) PPy-IC and (b) PPy-IC-Ag_{nanop} films in 0.1 mol L^{-1} $LiClO_4$ aqueous solution at a scan rate of 50 mV s^{-1}.

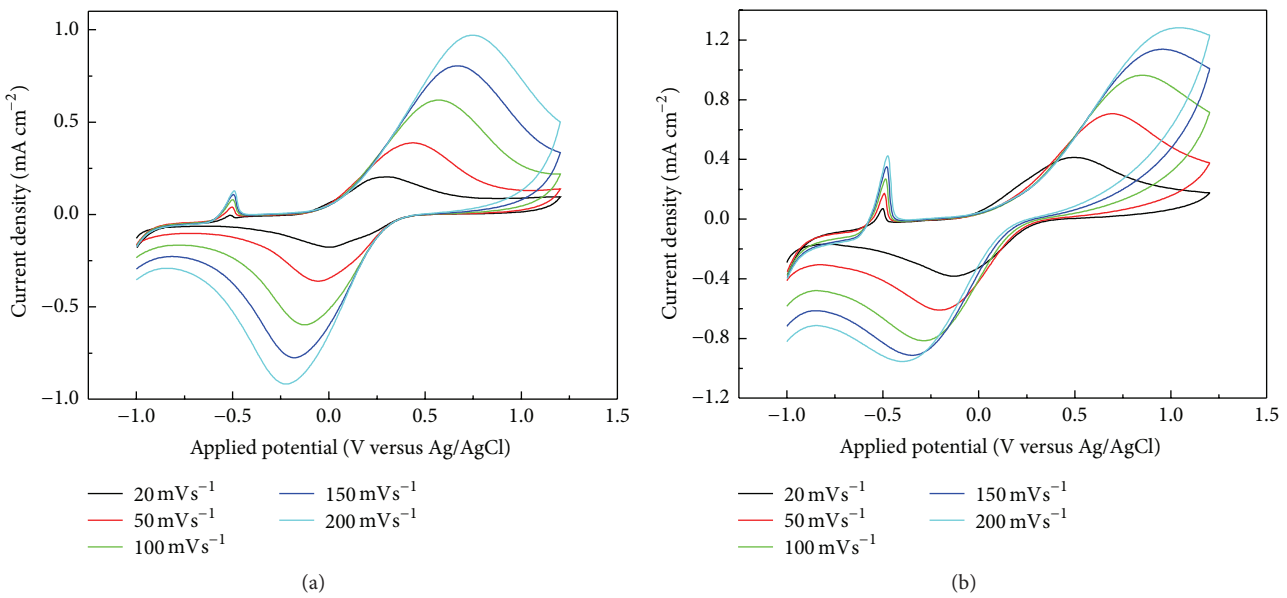

FIGURE 5: Voltammograms of (a) PPy-IC and (b) PPy-IC-Ag_{nanop} in 0.1 mol L^{-1} $LiClO_4$ solution at different scan rates.

of dopants on the nanoparticles surface may require ions from the electrolyte to compensate the charges generated during the redox process [39, 40]. Therefore, the presence of silver nanoparticles may avoid the dopant leaching but also creates a competition between doping and Ag nanoparticle stabilization.

The electrochemical bandgap energy of PPy-IC and PPy-IC-Ag_{nanop} was calculated by measuring the onset oxidation and reduction potentials from the voltammograms presented in Figure 4 [41–43]. The onset potentials for PPy-IC oxidation (E_{ox}) and reduction (E_{red}) are found at −0.127 V and 0.406 V, respectively; meanwhile for PPy-IC-Ag_{nanop} they are found at −0.067 V (E_{ox}) and 0.294 V (E_{red}). Hence, the electrochemical bandgaps of PPy-IC and PPy-IC-Ag_{nanop} were calculated as 0.53 eV and 0.36 eV, respectively, [31]. According to Brédas et al. [44], by increasing the conjugation length of the polymer chain one should observe a decrease in bandgap energy. Therefore the results obtained from the cyclic voltammetry corroborate the FTIR analysis suggesting that the presence of silver nanoparticles induces the polymerization of PPy chain with longer conjugation.

Table 1 summarizes the electrochemical parameters obtained from Figure 4. By comparing peak-to-peak separation (ΔE_p), formal potential [$(E_a + E_c)/2$], and the ratio between anodic and cathodic peaks ($|I_{pa}|/|I_{pc}|$) we can observe a good reversibility for both polymeric films [11, 45].

Figure 5 shows the voltammograms of PPy-IC and PPy-IC-Ag_{nanop} performed from −1.0 to +1.2 V in 0.1 M $LiClO_4$ at different scan rates. Both PPy-IC-Ag_{nanop} and PPy-IC present a pair of well-defined redox peaks, corresponding to the

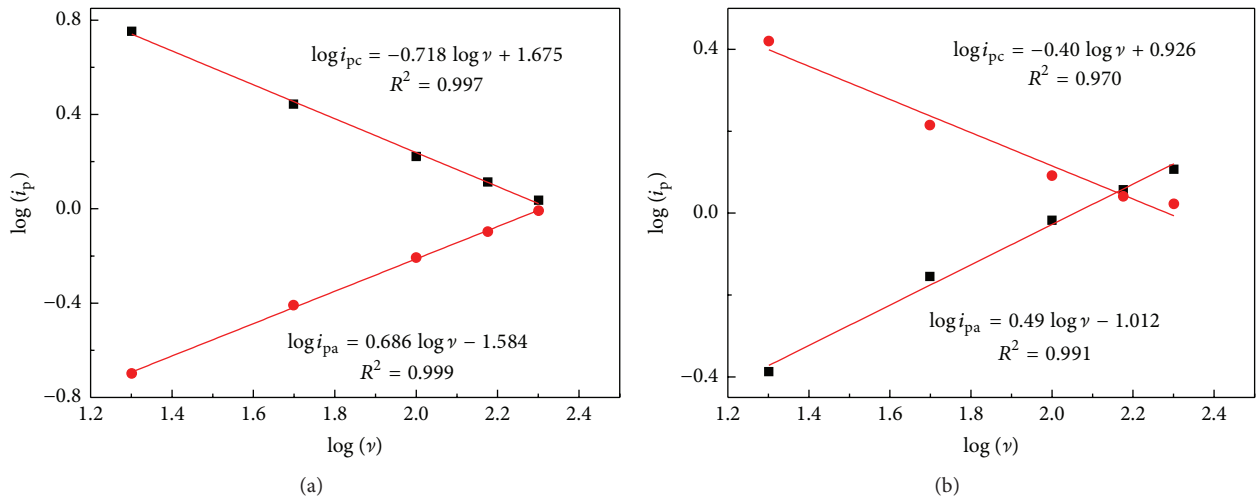

Figure 6: Plot of log i_p versus log scan rate for (a) PPy-IC and (b) PPy-IC-Ag_{nanop} films.

Table 1: Electrochemical parameters obtained from voltammograms of PPy-IC and PPy-IC-Ag_{nanop} (Figure 4).

Parameters	PPy-IC	PPy-IC-Ag_{nanop}
I_{pa} (mA cm^{-2})	0.20	0.41
E_{pa} (V)	0.30	0.55
I_{pc} (mA cm^{-2})	−0.18	−0.38
E_{pc} (V)	3.5×10^{-3}	−0.13
ΔE_p (V)	0.36	0.68
$(E_a + E_c/2)$	0.15	0.21
$\lvert I_{pa}\rvert/\lvert I_{pc}\rvert$	1.11	1.07

oxidation and reduction processes of polypyrrole [39, 40]. In both systems, as scan rate is increased, the anodic peak shifts to more positive potentials while the cathodic peak shifts toward the more negative direction. In addition, by increasing the scan rate, the cathodic peaks of PPy-IC-Ag_{nanop} became progressively broader in comparison to PPy-IC, suggesting that the cations and anions are no longer able to participate fully in the doping/dedoping process at high sweep rates [39].

The dependence of anodic and cathodic peaks on the scan rate was further evaluated in Figure 6, where the logarithm of the peak current (mA cm^{-2}) was plotted versus the logarithm of scan rate (mV s^{-1}) [45, 46]. The slopes for PPy-IC are 0.686 (anodic peak) and −0.718 (cathodic peak), with the correlation coefficients of 0.999 and 0.997, respectively (Figure 6(a)). For PPy-IC-Ag_{nanop} film (Figure 6(b)), the linear regression equations resulted in 0.490 (anodic peak) and −0.400 (cathodic peak) with the correlation coefficients of 0.991 and 0.970, respectively. Slopes close to 0.5 indicate a diffusional process as described by the Randles-Sevcik equation; meanwhile slopes close to 1.0 indicate a process controlled by the adsorption rate. Therefore, according to these results, the redox process in PPy-IC is partially controlled by diffusion [45] and, on the other hand, for PPy-IC-Ag_{nanop} the electrochemical process is controlled only by diffusion, indicating that the presence of silver nanoparticles facilitates the charge transfer between polymer chain and electrolyte [45, 47].

3.5. Electrocatalytic Activity of PPy-IC and PPy-IC-Ag_{nanop} Films for I_3^-/I^-. The electrochemical catalytic activities of PPy-IC and PPy-IC-Ag_{nanop} were tested for I_3^-/I^-, which is the main redox couple used to assemble Dye-Sensitized Solar Cells (DSSC). The cyclic voltammetry (Figure 7) was performed using a supporting electrolyte with 0.1 mol L^{-1} $LiClO_4$, 10 mmol L^{-1} NaI, and 1.0 mmol L^{-1} I_2 in acetonitrile. The redox peaks identified with asterisks are attributed to I_3^-/I^- redox reaction.

A higher current density was obtained from PPy-IC-Ag_{nanop} (Figure 7), indicating larger effective surface area [48]. Concerning the peak-to-peak separation and formal potential, both films presented lower positive values than the conventional platinum counter electrodes, indicating faster electron transfer kinetics or a greater electrocatalytic activity toward the I_3^-/I^- redox reaction for the polypyrrole films. This result is a consequence of a larger surface area for catalysis; therefore the materials developed in this work present potential to replace platinum for counter-electrode material in DSSC [25, 48].

3.6. Electrochromic Characterization of PPy-IC-Ag_{nanop} Film. Earlier reports show enhanced electrochromic properties obtained from nanocomposites of polypyrrole and gold nanoparticles, leading to higher optical contrast, fast response time, and good optical stability [11, 32, 49–51]. The optical contrast is the main electrochromic property to identify the electrochromic behavior of a material because it is a measurement of the transmittance variation ($\Delta\%T$) at a specified wavelength. In this work, the optical contrast was evaluated for the nanocomposite within 400 to 800 nm. According to Figure 8, the nanocomposite is an electrochromic material, presenting higher optical contrast

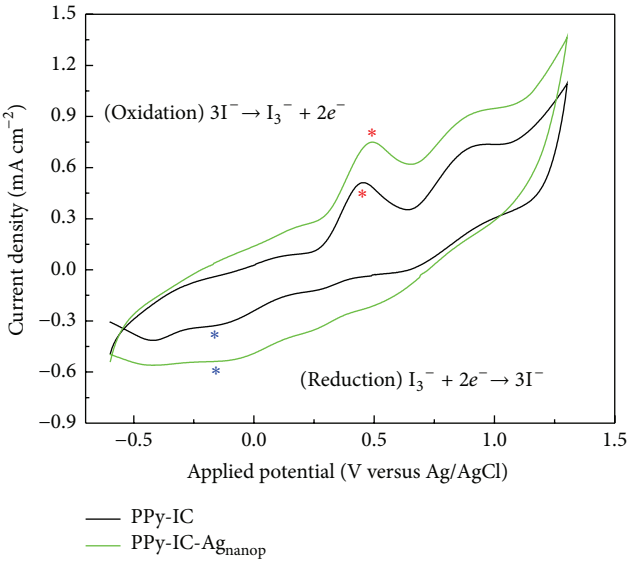

FIGURE 7: Voltammograms of I^-/I_3^- redox reaction at a scan rate of 20 mV s^{-1} on PPy-IC and PPy-IC-Ag$_{nanop}$ modified electrodes.

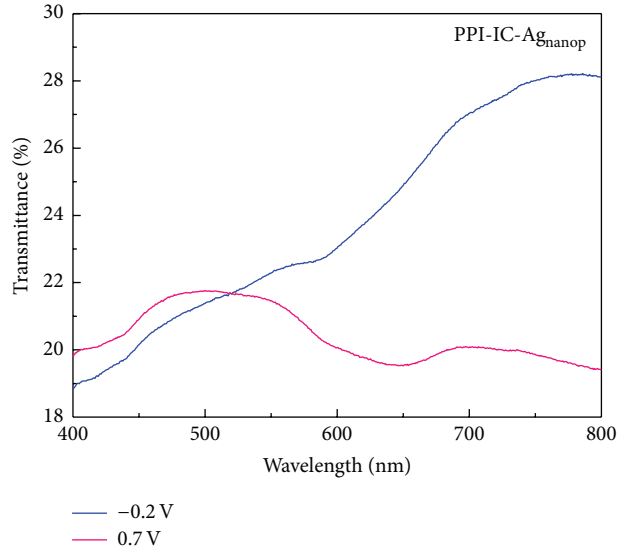

FIGURE 8: Optical contrast of PPy-IC-Ag$_{nanop}$ in 0.1 M $LiClO_4$ aqueous solution. The redox potentials (−0.2 V and 0.7 V) were applied for 90 s.

from 600 to 800 nm. The low optical contrast resulted in low coloration efficiency [11] and further studies on the amount of silver nanoparticles are necessary for improving the electrochromic properties.

4. Conclusions

We demonstrated a simple one-step electrochemical method to obtain a nanocomposite of silver nanoparticles embedded within a dye doped polypyrrole film. This method allows for increasing the conjugation length of the polymer chain, in addition to improving electroactivity. The nanocomposite synthesized in this work presents potential to be applied in electrochromic devices and as counter electrode in Dye-Sensitized Solar Cells and the methodology presented can be further studied to allow the characterization of a wide variety of conducting polymer-metal based nanocomposites, which could be exploited in the fabrication of novel and inexpensive devices.

Conflict of Interests

The authors declare that there is no conflict of interests regarding the publication of this paper.

Acknowledgments

The authors gratefully acknowledge funding support, scholarships, and fellowships from Conselho Nacional de Desenvolvimento Científico e Tecnológico (CNPq), Brazil, and Coordenação de Aperfeiçoamento de Pessoal de Nível Superior (CAPES). They are thankful to Center of Microscopy (CME-UFRGS) for the SEM images.

References

[1] E. Prodan, C. Radloff, N. J. Halas, and P. Nordlander, "A hybridization model for the plasmon response of complex nanostructures," *Science*, vol. 302, no. 5644, pp. 419–422, 2003.

[2] U. Kreibig and M. Vollmer, *Optical Properties of Metal Clusters*, Springer, Berlin, Germany, 1995.

[3] C. F. Bohren and D. R. Huffman, *Absorption and Scattering of Light by Small Particles*, Wiley-VCH, Weinheim, Germany, 1998.

[4] O. Masala and R. Seshadri, "Synthesis routes for large volumes of nanoparticles," *Annual Review of Materials Research*, vol. 34, pp. 41–81, 2004.

[5] Y. Han, J. Jiang, S. S. Lee, and J. Y. Ying, "Reverse microemulsion-mediated synthesis of silica-coated gold and silver nanoparticles," *Langmuir*, vol. 24, no. 11, pp. 5842–5848, 2008.

[6] H. Hiramatsu and F. E. Osterloh, "A simple large-scale synthesis of nearly monodisperse gold and silver nanoparticles with adjustable sizes and with exchangeable surfactants," *Chemistry of Materials*, vol. 16, no. 13, pp. 2509–2511, 2004.

[7] P. Dallas, D. Niarchos, D. Vrbanic et al., "Interfacial polymerization of pyrrole and in situ synthesis of polypyrrole/silver nanocomposites," *Polymer*, vol. 48, no. 7, pp. 2007–2013, 2007.

[8] W. Chen, C. M. Li, P. Ming Chen, and C. Q. Sun, "Electrosynthesis and characterization of polypyrrole/Au nanocomposite," *Electrochimica Acta*, vol. 52, no. 8, pp. 2845–2849, 2007.

[9] K. F. Babu, P. Dhandapani, S. Maruthamuthu, and M. A. Kulandainathan, "One pot synthesis of polypyrrole silver nanocomposite on cotton fabrics for multifunctional property," *Carbohydrate Polymers*, vol. 90, no. 4, pp. 1557–1563, 2012.

[10] F. Liu, Y. Yuan, L. Li et al., "Synthesis of polypyrrole nanocomposites decorated with silver nanoparticles with electrocatalysis and antibacterial property," *Composites Part B: Engineering*, vol. 69, pp. 232–236, 2014.

[11] L. F. Loguercio, C. C. Alves, A. Thesing, and J. Ferreira, "Enhanced electrochromic properties of a polypyrrole–indigo carmine–gold nanoparticles nanocomposite," *Physical Chemistry Chemical Physics*, vol. 17, no. 2, pp. 1234–1240, 2015.

[12] M. F. Ghadim, A. Imani, and G. Farzi, "Synthesis of PPy-silver nanocomposites via in situ oxidative polymerization," *Journal of Nanostructure in Chemistry*, vol. 4, article 101, 2014.

[13] M. Omastová, K. Mosnáčková, P. Fedorko, M. Trchová, and J. Stejskal, "Polypyrrole/silver composites prepared by single-step synthesis," *Synthetic Metals*, vol. 166, no. 1, pp. 57–62, 2013.

[14] X. Feng, "Synthesis of Ag/polypyrrole core-shell nanospheres by a seeding method," *Chinese Journal of Chemistry*, vol. 28, no. 8, pp. 1359–1362, 2010.

[15] M. Omastová, P. Bober, Z. Morávková et al., "Towards conducting inks: polypyrrole-silver colloids," *Electrochimica Acta*, vol. 122, pp. 296–302, 2014.

[16] J. Hazarika and A. Kumar, "Controllable synthesis and characterization of polypyrrole nanoparticles in sodium dodecylsulphate (SDS) micellar solutions," *Synthetic Metals*, vol. 175, pp. 155–162, 2013.

[17] Z. Gao, J. Bobacka, A. Lewenstam, and A. Ivaska, "Electrochemical behaviour of polypyrrole film polymerized in indigo carmine solution," *Electrochimica Acta*, vol. 39, no. 5, pp. 755–762, 1994.

[18] P. R. Somani and S. Radhakrishnan, "Electrochromic materials and devices: present and future," *Materials Chemistry and Physics*, vol. 77, no. 1, pp. 117–133, 2003.

[19] I. Sultana, M. M. Rahman, J. Wang, C. Wang, G. G. Wallace, and H.-K. Liu, "Indigo carmine (IC) doped polypyrrole (PPy) as a free-standing polymer electrode for lithium secondary battery application," *Solid State Ionics*, vol. 215, pp. 29–35, 2012.

[20] Y. Wei, L. Li, X. Yang, G. Pan, G. Yan, and X. Yu, "One-step UV-induced synthesis of polypyrrole/Ag nanocomposites at the water/ionic liquid Interface," *Nanoscale Research Letters*, vol. 5, no. 2, pp. 433–437, 2010.

[21] R. Gupta, K. Jayachandran, J. S. Gamare, B. Rajeshwari, S. K. Gupta, and J. V. Kamat, "Novel electrochemical synthesis of polypyrrole/ag nanocomposite and its electrocatalytic performance towards hydrogen peroxide reduction," *Journal of Nanoparticles*, vol. 2015, Article ID 149406, 6 pages, 2015.

[22] M. Nakata, M. Taga, and H. Kise, "Synthesis of electrical conductive polypyrrole films by interphase oxidation polymerization—effects of polymerization temperature and oxidizing agents," *Polymer Journal*, vol. 24, no. 5, pp. 437–441, 1992.

[23] S. Singh, D. V. S. Jain, and M. L. Singla, "One step electrochemical synthesis of gold-nanoparticles-polypyrrole composite for application in catechin electrochemical biosensor," *Analytical Methods*, vol. 5, no. 4, pp. 1024–1032, 2013.

[24] E. M. Girotto and M.-A. De Paoli, "Polypyrrole color modulation and electrochromic contrast enhancement by doping with a dye," *Advanced Materials*, vol. 10, no. 10, pp. 790–793, 1998.

[25] S. Lu, X. Zhang, T. Feng, R. Han, D. Liu, and T. He, "Preparation of polypyrrole thin film counter electrode with pre-stored iodine and resultant influence on its performance," *Journal of Power Sources*, vol. 274, pp. 1076–1084, 2015.

[26] J. Ding, K. Zhang, G. Wei, and Z. Su, "Fabrication of polypyrrole nanoplates decorated with silver and gold nanoparticles for sensor applications," *RSC Advances*, vol. 5, no. 85, pp. 69745–69752, 2015.

[27] J. K. Gan, Y. S. Lim, N. M. Huang, and H. N. Lim, "Hybrid silver nanoparticle/nanocluster-decorated polypyrrole for high-performance supercapacitors," *RSC Advances*, vol. 5, no. 92, pp. 75442–75450, 2015.

[28] S. Xing and G. Zhao, "One-step synthesis of polypyrrole-Ag nanofiber composites in dilute mixed CTAB/SDS aqueous solution," *Materials Letters*, vol. 61, no. 10, pp. 2040–2044, 2007.

[29] R. C. Chikate and B. S. Kadu, "Improved photocatalytic activity of CdSe-nanocomposites: effect of Montmorillonite support towards efficient removal of Indigo Carmine," *Spectrochimica Acta—Part A, Molecular and Biomolecular Spectroscopy*, vol. 124, pp. 138–147, 2014.

[30] M. Chang, T. Kim, H.-W. Park, M. Kang, E. Reichmanis, and H. Yoon, "Imparting chemical stability in nanoparticulate silver via a conjugated polymer casing approach," *ACS Applied Materials and Interfaces*, vol. 4, no. 8, pp. 4357–4365, 2012.

[31] J. L. Brédas, J. C. Scott, K. Yakushi, and G. B. Street, "Polarons and bipolarons in polypyrrole: evolution of the band structure and optical spectrum upon doing," *Physical Review B*, vol. 30, no. 2, pp. 1023–1025, 1984.

[32] F. Tavoli and N. Alizadeh, "In situ UV-vis spectroelectrochemical study of dye doped nanostructure polypyrrole as electrochromic film," *Journal of Electroanalytical Chemistry*, vol. 720-721, pp. 128–133, 2014.

[33] M. Choudhary, S. Siwal, and K. Mallick, "Single step synthesis of a 'silver–polymer hybrid material' and its catalytic application," *RSC Advances*, vol. 5, no. 72, pp. 58625–58632, 2015.

[34] M. Joulazadeh and A. H. Navarchian, "Polypyrrole nanotubes versus nanofibers: a proposed mechanism for predicting the final morphology," *Synthetic Metals*, vol. 199, pp. 37–44, 2015.

[35] J. L. Brédas, B. Thémans, and J. M. André, "Bipolarons in polypyrrole chains," *Physical Review B*, vol. 27, no. 12, pp. 7827–7830, 1983.

[36] J. L. Brédas and G. B. Street, "Polarons, bipolarons, and solitons in conducting polymers," *Accounts of Chemical Research*, vol. 18, no. 10, pp. 309–315, 1985.

[37] A. L. C. M. de Silva, M. G. Gutierres, A. Thesing, R. M. Lattuada, and J. Ferreira, "SPR biosensors based on gold and silver nanoparticle multilayer films," *Journal of the Brazilian Chemical Society*, vol. 25, no. 5, pp. 928–934, 2014.

[38] C. A. Rodrigues, E. Stadler, M. C. M. Laranjeira, and V. Drago, "The preparation and characterization of the hexacyanides immobilized in chitosan," *Journal of the Brazilian Chemical Society*, vol. 8, no. 1, pp. 7–11, 1997.

[39] M. A. Careem, Y. Velmurugu, S. Skaarup, and K. West, "A voltammetry study on the diffusion of counter ions in polypyrrole films," *Journal of Power Sources*, vol. 159, no. 1, pp. 210–214, 2006.

[40] S. Skaarup, L. Bay, K. Vidanapathirana, S. Thybo, P. Tofte, and K. West, "Simultaneous anion and cation mobility in polypyrrole," *Solid State Ionics*, vol. 159, no. 1-2, pp. 143–147, 2003.

[41] A. Misra, P. Kumar, R. Srivastava, S. K. Dhawan, M. N. Kamalasanan, and S. Chandra, "Electrochemical and optical studies of conjugated polymers for three primary colours," *Indian Journal of Pure and Applied Physics*, vol. 43, no. 12, pp. 921–925, 2005.

[42] A. Shafiee, M. M. Salleh, and M. Yahaya, "Determination of HOMO and LUMO of [6,6]-phenyl C61-butyric acid 3-ethylthiophene ester and poly (3-octyl-thiophene-2, 5-diyl) through voltametry characterization," *Sains Malaysiana*, vol. 40, no. 2, pp. 173–176, 2011.

[43] J. C. Bernède, A. Godoy, L. Cattin, F. R. Diaz, M. Morsli, and M. A. del Valle, "Organic solar cells performances improvement induced by interface buffer layers," in *Solar Energy*, R. D. Rugescu, Ed., pp. 223–266, InTech, Rijeka, Croatia, 2010.

[44] J. L. Brédas, R. Silbey, D. S. Boudreaux, and R. R. Chance, "Chain-length dependence of electronic and electrochemical properties of conjugated systems: polyacetylene, polyphenylene, polythiophene, and polypyrrole," *Journal of the American Chemical Society*, vol. 105, no. 22, pp. 6555–6559, 1983.

[45] R. A. Zoppi and M. A. De Paoli, "Electrochemical characterization of polypyrrole and polypyrrole/EPDM rubber blends by cyclic voltammetry and impedancimetry," *Journal of The Brazilian Chemical Society*, vol. 5, no. 3, pp. 197–201, 1994.

[46] D. Pamuk, İ. H. Taşdemir, A. Ece, E. Canela, and E. Kılıç, "Redox pathways of aliskiren based on experimental and computational approach and its voltammetric determination," *Journal of the Brazilian Chemical Society*, vol. 24, pp. 1276–1286, 2013.

[47] X. Feng, H. Huang, Q. Ye, J.-J. Zhu, and W. Hou, "Ag/polypyrrole core-shell nanostructures: interface polymerization, characterization, and modification by gold nanoparticles," *The Journal of Physical Chemistry C*, vol. 111, no. 24, pp. 8463–8468, 2007.

[48] S. S. Jeon, C. Kim, J. Ko, and S. S. Im, "Pt nanoparticles supported on polypyrrole nanospheres as a catalytic counter electrode for dye-sensitized solar cells," *The Journal of Physical Chemistry C*, vol. 115, no. 44, pp. 22035–22039, 2011.

[49] J. Ferreira, M. J. L. Santos, R. Matos, O. P. Ferreira, A. F. Rubira, and E. M. Girotto, "Structural and electrochromic study of polypyrrole synthesized with azo and anthraquinone dyes," *Journal of Electroanalytical Chemistry*, vol. 591, no. 1, pp. 27–32, 2006.

[50] J. Zhang, J.-P. Tu, D. Zhang et al., "Multicolor electrochromic polyaniline–WO_3 hybrid thin films: one-pot molecular assembling synthesis," *Journal of Materials Chemistry*, vol. 21, no. 43, pp. 17316–17324, 2011.

[51] B. Yigitsoy, S. Varis, C. Tanyeli, I. M. Akhmedov, and L. Toppare, "Electrochromic properties of a novel low band gap conductive copolymer," *Electrochimica Acta*, vol. 52, no. 23, pp. 6561–6568, 2007.